New Journal of Physics
The open access journal at the forefront of physics
Deutsche Physikalische Gesellschaft DPG | IOP Institute of Physics

Using the third state of matter: high harmonic generation from liquid targets

P Heissler[1], E Lugovoy[2,4], R Hörlein[1], L Waldecker[1], J Wenz[1], M Heigoldt[1], K Khrennikov[1], S Karsch[1], F Krausz[1,3], B Abel[2,4] and G D Tsakiris[1]

[1] Max-Planck-Institut für Quantenoptik, D-85748, Garching, Germany
[2] Wilhelm-Ostwald-Institut für Physikalische und Theoretische Chemie, Leipzig Universität, Linnéstr. 2, D-04103, Leipzig, Germany
[3] Fakultät für Physik, Ludwig-Maximilians-Universität München, D-85748, Garching, Germany
[4] Leibniz-Institut für Oberflächenmodifizierung, Chemische Abteilung, Permoserstr. 15, D-04318, Leipzig, Germany
E-mail: info@patrick-heissler.de

Received 9 July 2014, revised 26 August 2014
Accepted for publication 3 October 2014
Published 20 November 2014

New Journal of Physics **16** (2014) 113045

doi:10.1088/1367-2630/16/11/113045

Abstract

High harmonic generation on solid and gaseous targets has been proven to be a powerful platform for the generation of attosecond pulses. Here we demonstrate a novel technique for the XUV generation on a smooth liquid surface target in vacuum, which circumvents the problem of low repetition rate and limited shot numbers associated with solid targets, while it maintains some of its merits. We employed atomically smooth, continuous liquid jets of water, aqueous salt solutions and ethanol that allow uninterrupted high harmonic generation due to the coherent wake emission mechanism for over 8 h. It has been found that the mechanism of plasma generation is very similar to that for smooth solid target surfaces. The vapor pressure around the liquid target in our setup has been found to be very low such that the presence of the gas phase around the liquid jet could be neglected.

Keywords: attosecond physics, relativistic laser–plasma interaction, liquid jets, high harmonic generation

Introduction

The coherent interaction of a high intensity laser pulse with a solid density surface is currently a topic of intense investigations in high field laser laboratories with a number of applications. Focusing high intensity laser pulses with high temporal contrast onto solid targets can lead to the generation of high harmonics of the laser frequency and very high intensity light pulses on the attosecond (as, 10^{-18} s) time scale [1, 2]. Due to the high intensity of the driving laser pulse and a high conversion efficiency [3] these pulses are expected to be orders of magnitude more intense than that of high power short pulse laser systems [4]. But they require high quality unspoiled interaction surfaces, making it necessary to supply a fresh area of target after every shot. Conventionally used glass plate targets last only for a few hundred up to a few thousand shots, depending on target and damage spot size, before they have to be replaced, in contrast to state of the art as-pulse sources on the basis of gaseous media [5]. Advances in high intensity laser technology towards ever higher repetition rates and their first applications [6, 7] urgently call for new target concepts. Especially in the prospect of large scale user facilities like ELI [8] this is a critical task for making the transition from pure exploration of these new as-sources to their application in e.g. XUV pump–probe type experiments. Promising candidates for a self-replenishing target with no limitations on the maximum shot number are smooth jets of liquids [9–11]. After the first demonstration of liquid jets as targets for plasma mirrors [12] several experiments using this concept have already been performed [13, 14]. However these experiments have been carried out under rough vacuum (50 Torr) [13] or even atmospheric pressure [14], limiting the focused laser power to below 10^{14} W cm^{-2}.

In order to extend the usable laser power to intensities high enough for applications, we study the interaction of high power laser pulses with an atomically smooth liquid surface aiming at high harmonic generation in vacuum. This broadband, coherent emission is in many aspects different from previous experiments with liquid jets generating quasimonochromatic, incoherent XUV radiation [15]. Two mechanisms are known to contribute to the generation of harmonic radiation off solid surfaces. One is known as coherent wake emission (CWE) and described in detail in [2, 16, 17]. CWE is in general dominant for laser intensities where relativistic effects can be neglected. At higher intensities the relativistically oscillating mirror (ROM) mechanism is prevalent [18–21]. By looking at the highest harmonic generated, it is possible to immediately distinguish between the two mechanisms. Since in the CWE process plasma waves produce the XUV radiation, no light at frequencies higher than the plasma frequency ω_P of the target material can be emitted. In contrast to this clear cut-off in the CWE mechanism, in the ROM mechanism, which can be described by relativistic Doppler upshifting, the highest observable harmonics are determined by the focused intensity of the driving laser and occur rather in a smooth roll-off than in a clear cut-off.

Experimental setup

For our experiments we use the ATLAS laser system at the Max-Planck-Institute of Quantum Optics. It is capable of delivering pulses of up to 2 J in energy with duration down to 26 fs at 800 nm central wavelength. They are focused by a high quality *f*/2 parabolic mirror to a spot size of ~8 μm. The liquid enters the interaction chamber through a convergent, circular quartz nozzle (Microliquids GmbH) with a typical aperture on the order of 10–20 μm. The nozzle is

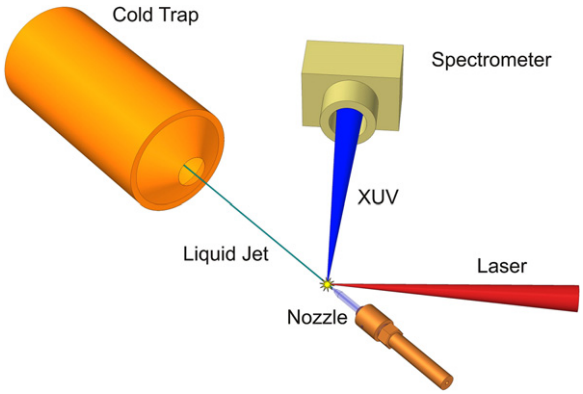

Figure 1. Experimental setup. The laser is focused on a continuously flowing liquid target under an angle of 45°. The specularly reflected light is analyzed by a XUV spectrometer.

mounted in a horizontal configuration at an angle of 45° to the focusing laser beam. The continuously flowing liquid jet propagates freely through the vacuum chamber for ≈10 cm and is then collected in a double walled liquid nitrogen cold trap (see figure 1). Using such a cold trap, a pressure on the order of 10^{-5} mbar can be maintained in the interaction chamber during jet operation. The volume capacity of this cold trap is the only limiting factor for the duration of operation of the jet. In our case, depending on nozzle size and flow rate of the liquid, more than 8 h of uninterrupted experimental time is available. By using a high pressure liquid chromatography pump a steady operation of the jet can be maintained while the temperature of the liquid is controlled by a cryostat. The specularly reflected light is then analyzed by a XUV-spectrometer (Acton VM-502) where single shots as well as accumulated spectra are recorded.

In previous experiments with solid state targets [22] we have found that for effective generation of high harmonics the roughness of the sample surface should be below 20 nm. A liquid jet emerging from a circular nozzle propagates as a smooth cylindrical laminar flow filament until it breaks up into droplets at distances of several millimeters downstream of the nozzle. To effectively generate high harmonics the laser focus should be placed on this laminar part of the jet.

Choosing the target material out of a number of available liquids some constraints have to be kept in mind. The liquid should be non-toxic and easy to handle. But most importantly, the vapor pressure should be low enough to minimize gas phase absorption of the incoming laser radiation and especially re-absorption of outgoing XUV light.

In this work we perform several runs with three different liquids in the form of a high-pressure liquid micro-jet in vacuum: pure water, an aqueous solution of LiCl and ethanol.

Results and discussion

With all three materials the generation of high order harmonics of the driving laser frequency is possible (see figure 2). Although we cannot observe the cut-off of the CWE process (see table 1) due to the spectral range of the spectrometer, we conclude that under the present experimental conditions the harmonics appear to be produced solely by the CWE mechanism.

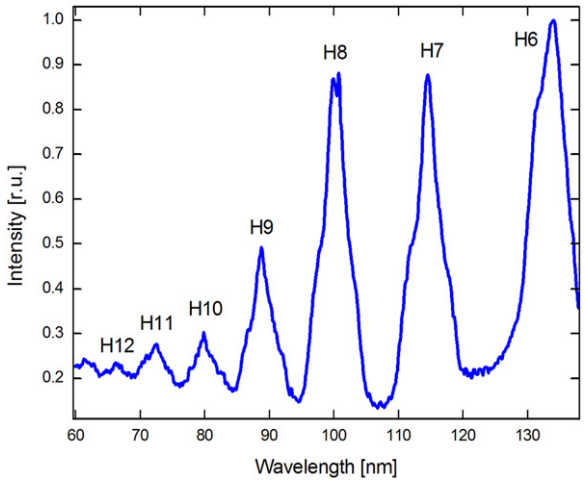

Figure 2. Accumulated spectrum of ≈150 shots with ≈200 mJ of laser energy on target on an aqueous solution of LiCl at −15 °C.

Table 1. Temperature, vapor pressure, mean free path of evaporated molecules directly under the nozzle (T_0, P_0 and λ_0) and at the position of the laser focus 3 mm away from the orifice of the nozzle (T_F, P_F and λ_F). Relative number of molecules evaporated from the jet (vapor fraction) and expected highest harmonic by the CWE mechanism are also shown. Nozzle ø 17 μm (jet ø 13 μm), flow rate of 0.4 ml min^{-1}.

	T_0(C)	P_0(mbar)	λ_0(μm)	T_F(C)	P_F(mbar)	λ_F(μm)	Vapor fraction	Highest CWE harmonic
H_2O	0	6.1	21	−21.6	1.2	97	0.53	14
	3	7.5	17	−20.0	1.3	93	0.60	
	6	9.3	14	−19.6	1.3	90	0.66	
	9	11	11	−19.2	1.3	87	0.73	
	12	14	9	−18.9	1.4	85	0.80	
	15	17	7.8	−18.6	1.4	83	0.86	
	18	21	6.5	−18.4	1.4	82	0.93	
	21	25	5.5	−18.2	1.5	80	1.00	
H_2O/LiCl	−15	1.5	81	−23.5	0.72	159	0.21	20
Ethanol	−25	2.1	19	−38.0	0.66	57	0.24	12

The very weak dependence of the harmonic signal on laser intensity and target position, which is characteristic of the CWE mechanism and in strong contrast compared to observations with ROM harmonics off glass targets [23], leads to this statement. Notwithstanding the ability to generate harmonics off any of the three investigated liquids, they show a large difference in XUV generation efficiency and handling during the experiments.

Water, as the most obvious candidate, shows overall very good performance in terms of stability and high harmonic generation. By cooling the water from 21 °C down to 0 °C the harmonic signal can be enhanced by a factor of ≈2 (see figure 3). The most significant difference is observed by changing the temperature from 6 °C to 0 °C. Adding LiCl to the water (solute mass fraction of 0.15 or 176 g of LiCl in 1 l of water), leads, according to Blagden's law, to the depression of the freezing point to −15 °C [24] and the reduction of the vapor pressure by

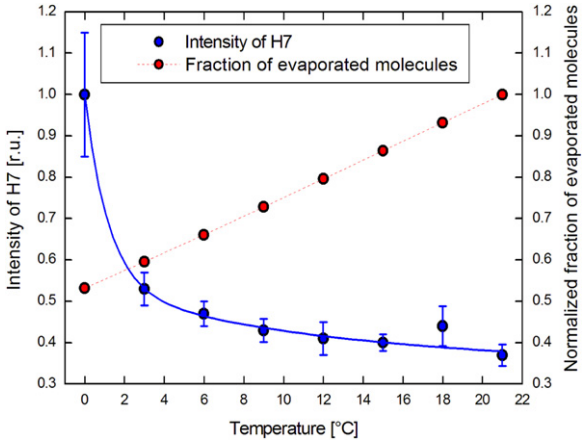

Figure 3. Temperature dependence of intensity of harmonic 7 using water as a target. (Nozzle diameter of 17 μm, flow rate of 0.4 ml min^{-1}). Relative number of evaporated molecules is shown as a dash line (see text).

a factor of 0.78 [25]. Indeed an aqueous solution of LiCl shows improved performance over pure water. The harmonic signal strength increases by going down to −15 °C. A major drawback for the use of this liquid is the formation of Li^+ and Cl^- ions in the laser focus. These ion species effectively corrode most surfaces, including optics, within the vacuum chamber. This results in damaged optical coatings as well as battered mechanical parts.

The freezing point of the third liquid under consideration, ethanol, at −114 °C allows for even lower temperatures of operation and accompanying low vapor pressures. This should lead to even better performance in terms of harmonic generation. The low freezing point at the same time also hinders the efficient trapping of the liquid within the cold trap which leads to a higher pressure, in the 10^{-4} mbar range, in the vacuum chamber and unpredictable, sudden jumps of the chamber pressure.

For the analysis of the observed results and definition of optimal conditions for most effective generation of coherent XUV light using liquid jets the vapor pressure and as a result the trajectories and mean free paths of evaporated molecules play the key role. To simplify the discussion we take into account only one set of experiments with a nozzle diameter of 17 μm and a flow rate of 0.4 ml min^{-1}.

For efficient flow from a molecular source the mean free path λ of evaporated molecules should be larger than the size of the source d (Knudsen condition). Here we may assume that evaporated molecules have ballistic, collision free trajectories directed, in average, perpendicular to the liquid.

A liquid jet emerging from a nozzle contracts within a distance of a few nozzle diameters to its final cross section d. The jet contraction primarily depends on the nozzle shape [26]. For the nozzle in use, a water jet diameter of 13 μm was measured using HeNe laser diffraction.

Evaporation of molecules from the free surface of the liquid jet introduced in vacuum leads to a decrease of its temperature. We use a simple one-dimensional model [10] to estimate the evaporation cooling rates as well as the density of the vapor phase surrounding the jet (see appendix for details). Values of the enthalpies of vaporization and specific heats used in the simulation were taken from [27] and [28]. For jet diameters of the order of 10–20 μm and velocities of 20–30 m s^{-1} the model gives a cooling rate of 10^5 K s^{-1} in the initial section of the

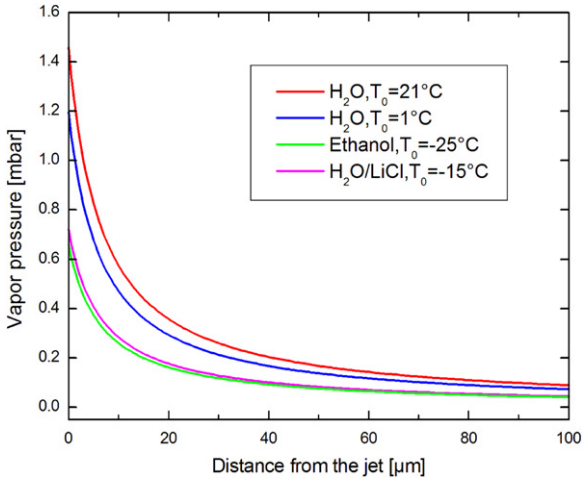

Figure 4. Variation of vapor pressure at the laser focus plane (3 mm below the nozzle) in normal direction to the jet.

liquid jet. This implies that the most significant temperature change and the most active evaporation takes place on the first millimeter of the jet.

In our experiments the laser is focused on the jet at a distance of ≈3 mm from the nozzle. Depending on the initial temperature (T_0), the type of the liquid and the jet velocity, the temperature of the jet at the interaction point (T_F) as well as the vapor pressure and mean free path of evaporated molecules may vary. The relative number of evaporated molecules (vapor fraction) was calculated at a distance of 3 mm. For longer distances the final result does not change noticeably. In case of ballistic trajectories, the local pressure of evaporated molecules should decrease with distance R from the jet as $1/R$ to the background pressure in the vacuum chamber (see figure 5).

The results of calculations are summarized in table 1 and figure 4. Although the drop of the vapor fraction from a factor of 1.0–0.53 by decreasing the water temperature from 21 °C to 0 °C corresponds to the rise of the intensity of HH7 shown on figure 3, the Knudsen condition for molecules evaporated directly at the nozzle is reached only for an initial liquid temperature below 6 °C. For higher temperatures the molecules remain longer nearby the jet and form an additional 'vapor shielding' due to collisions. This leads to absorption of XUV light and a decrease of the observed intensity. This conclusion is in good agreement with the experimental data.

A very important parameter for the generation of high order harmonics is the scale length of the formed plasma [29, 30]. It describes the distance of the critical density surface, the point of reflection of the laser off the plasma, from the liquid surface. For all three materials the critical density, given by $n_c = \omega_0^2 m_e \varepsilon_0 / e^2$ with ω_0 frequency of incoming radiation, e electronic charge, m_e electron mass and ε_0 permittivity of free space, for 800 nm wavelength is about 5 orders of magnitude higher than the density of the vapor surrounding the jet. Hence, as soon as the Knudsen condition is reached, the laser has to traverse an under-dense plasma region of several microns length but then interacts, similarly to the solid target case, with a very smooth over-dense surface. As in the case of solid density targets the scale length of the plasma is therefore only affected by the laser parameters, i.e. the temporal contrast of the high intensity

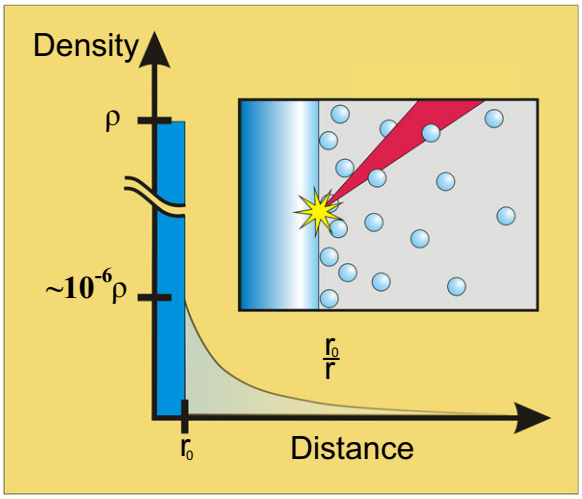

Figure 5. Schematic diagram of the liquid phase and vapor phase density ρ as a function of distance from the jet. Here ρ is density of the liquid and r_0 is the radius (surface) of the jet.

laser pulse. Hence, ROM generation on these smooth liquid surfaces is possible, but could not be confirmed in our experiments due to the limitations of the used spectrometer.

Another question is which geometrical factors decrease the efficiency of the high harmonic generation and their subsequent transport. First of all it should be noted that a simple cooling trap used in the present experiments loses its efficiency after several hours of work. Formation of a thick layer of ice inside the trap leads to backflow of vapor that reduces the stability of the jet and leads to ice formation on the outside of the cooling trap. Over time this frozen liquid starts to form sticks of ice at the entrance of the cold trap. These sticks grow along the incoming water jet, eventually reaching the nozzle, freezing it up and preventing further jet operation.

To minimize the gas flow out of the trap and prevent ice formation, a trap equipped with a skimmer with an entrance orifice of 0.1–0.5 mm [11] can be employed. Another factor reducing the harmonic signal in the spectrometer results from geometrical considerations and is common for all liquids in use. For our studies we used circular nozzles with diameters of 12–27 μm to generate the liquid jet. These nozzles are hence producing circular symmetric jets with diameters of 8–20 μm. The size of the focal spot of the laser beam is also on the scale of a few μm. Small fluctuations in the backing pressure of the jet or tiny movements of optical parts in the laser beam line lead to μm jitter of the position of the jet relative to the focal spot. These μm deviations of the perfect alignment of the laser on the cylindrical surface of the jet cause strong deflections of the reflected light off the optical axis, and consequently reduce the collected signal seen by the spectrometer. This can only be circumvented by the use of larger diameter nozzles, which increase the gas load in the interaction chamber, or the use of flat jets—which are under development in our laboratory at present.

In summary, we demonstrated for the first time the generation of high-order harmonics around 100 nm wavelength off continuously flowing liquid targets (water, aqueous salt solutions, and ethanol). It has been found that the mechanism of plasma generation is very similar to that for smooth solid target surfaces. The harmonic emission can be efficiently

increased by lowering the vapor pressure of the liquid. The vapor pressure around the liquid target is low enough that the presence of the gas phase around the liquid jet can be neglected for the mechanism of high harmonic generation. Moreover, the liquid surface appears to be much smoother than it is required for efficient generation of relativistic harmonics. Given the present results on high vapor pressure liquid jets it is also possible to think about and apply cryogenic liquid cryo-jets with liquefied (noble) gases. The only problem at this stage appears to be the geometry of the liquid beam, i.e., its round shape. Our results are very promising for the use of these targets in further applications but additional investigations in target materials and nozzle configurations are necessary. Flat liquid jets in vacuum—which are currently under development—hold exciting prospects for future high harmonics applications.

Acknowledgments

BA and EL acknowledge discussions with Dr A Charvat and financial support from the IOM Leipzig as well as the University of Leipzig. This work was funded in part by DFG projects TR-18, by MAP excellence cluster, by LASERLAB II Europe, grant agreement no. 228334 and by the Associations EURATOM-MPI für Plasmaphysik and EURATOM.

Appendix

Evaporative cooling model

The simple model of jet evaporative cooling in vacuum was developed by M Faubel *et al* [10] and based on liquid/vapor energy balance:

$$\mathrm{d}T_0 = -\alpha \frac{H}{C_\mathrm{p}}, \tag{1}$$

where $\mathrm{d}T_0$ is an infinitesimal temperature decrease, H is the heat of vaporization, C_p—the specific heat capacity of the liquid and α the ratio of the number of molecules which have evaporated to those remaining the jet.

As it was shown in [10], for cylindrical filament equation (1) transforms to a spatial variation of temperature along the z axis:

$$\frac{\mathrm{d}T_0}{\mathrm{d}z} = -\frac{2}{v_\mathrm{jet}} \frac{H}{C_\mathrm{p}} \frac{1}{r_0} \frac{\mathrm{d}r_0}{\mathrm{d}t}, \tag{2}$$

where v_jet is velocity of the liquid jet and

$$\frac{\mathrm{d}r_0}{\mathrm{d}t} = -u\left(T_0\right) \frac{\rho_\mathrm{vapor}\left(T_0\right)}{\rho_\mathrm{liquid}}, \tag{3}$$

$$u\left(T_0\right) = \sqrt{\frac{8kT}{\pi m}} \tag{4}$$

are the rate of decrease of the jet radius and the mean velocity for the evaporating molecules respectively. For a two phase liquid–vapor system, the vapor density dependence on the liquid temperature T_0 is represented by Clausius–Clapeyron relation:

$$\rho_{\text{vapor}} = \text{Const} \times \exp\left(-\frac{H}{RT}\right). \tag{5}$$

A constant in the last equation may be found using known values of vapor density and head of vaporization for a fixed reference temperature (T_{ref}). For instance, in the present work $T_{\text{ref}} = 273.15$ K, $H(T_{\text{ref}}) = 45051$ J mol^{-1}, $\rho_{\text{liquid}}(T_{\text{ref}}) = 1 \times 10^6$ g m^{-3} and $\rho_{\text{vapor}}(T_{\text{ref}}) = 4.85$ g m^{-3} [28] were used. It also should be noted that the ratio of the enthalpy of vaporization and the heat capacity is nearly constant over the entire temperature range studied and both these parameters may be assumed in equation (2) as independent of T_0.

Mean free path calculation

The mean free path of evaporated molecule was calculated by formula:

$$\lambda(T) = \frac{1}{\sqrt{2}\pi \times \sigma_{\text{coll}}^2 \times \rho_{\text{vapor}}(T)}, \tag{6}$$

where σ_{coll} is the collision diameter of water (2.6×10^{-10} m) or ethanol (4.4×10^{-10} m) [31].

For practical use it is more convenient to present equation (6) in form:

$$\lambda(T)(\mu\text{m}) = \frac{0.46 \times T\,(\text{K})}{P\,(\text{mbar})} \tag{6a}$$

for water

and

$$\lambda(T)(\mu\text{m}) = \frac{0.16 \times T\,(\text{K})}{P\,(\text{mbar})} \tag{6b}$$

for ethanol.

References

[1] Nomura Y *et al* 2008 Attosecond phase locking of harmonics emitted from laser produced plasmas *Nat. Phys.* **5** 124–8

[2] Heissler P *et al* 2010 Toward single attosecond pulses using harmonic emission from solid density plasmas *Appl. Phys.* B **101** 511–21

[3] Tsakiris G D, Eidmann K, Meyer-ter-Vehn J and Krausz F 2006 Route to intense single attosecond pulses *New J. Phys.* **8** 19

[4] Ferrari F, Calegari F, Lucchini M, Vozzi C, Stagira S, Sansone G and Nisoli M 2010 High-energy isolated attosecond pulses generated by above-saturation few-cycle fields *Nat. Photonics* **4** 875–9

[5] Dromey B, Kar S, Zepf M and Foster P 2004 The plasma mirror. A subpicosecond optical switch for ultrahigh power lasers *Rev. Sci. Instrum.* **75** 645

[6] Borot A *et al* 2011 High-harmonic generation from plasma mirrors at kilohertz repetition rate *Opt. Lett.* **36** 1461–3

[7] Shaw B H *et al* 2013 *J. Appl. Phys.* **114** 043106

[8] Chambaret J-P *et al* 2010 Extreme light infrastructure: laser architecture and major challenges *Proc. SPIE* **7721** 77211D

[9] Faubel M and Kisters T 1989 Non-equilibrium molecular evaporation of carboxylic acid dimers *Nature* **339** 527–9

[10] Faubel M, Schlemmer S and Toennies J P 1988 A molecular beam study of the evaporation of water from a liquid jet *Z. Phys.* D **10** 269–77
[11] Charvat A, Lugovoj E, Faubel M and Abel B 2004 New design for a time-of-flight mass spectrometer with a liquid beam laser desorption ion source for the analysis of biomolecules *Rev. Sci. Instrum.* **75** 1209
[12] Backus S, Kapteyn H C, Murnane M M, Gold D M, Nathel H and White W 1993 Prepulse suppression for high-energy ultrashort pulses using self-induced plasma shuttering from a fluid target *Opt. Lett.* **18** 134–6
[13] Panasenko D, Shu A J, Gonsalves A, Nakamura K, Matlis N H, Toth C and Leemans W P 2010 Demonstration of a plasma mirror based on a laminar flow water film *J. Appl. Phys.* **108** 044913
[14] Panasenko D *et al* 2009 Staging laser plasma accelerators for increased beam energy *Proc. 13th Advanced Accelerator Concepts Workshop* ed C B Schroeder, W Leemans and E Esarey pp 215–20
[15] Kim B, Ahn B, Lee D, Kim J and Kim D 2006 Optimization of laser parameters for the maximum efficiency in the generation of water-window radiation using a liquid nitrogen jet *Appl. Phys. Lett.* **88** 141501
[16] Quéré F, Mairesse Y and Itatani J 2005 Temporal characterization of attosecond XUV fields *J. Mod. Opt.* **52** 339–60
[17] Thaury C *et al* 2007 Plasma mirrors for ultrahigh-intensity optics *Nat. Phys.* **3** 424–9
[18] Lichters R, Meyer-ter-Vehn J and Pukhov A 1996 Short pulse laser harmonics from oscillating plasma surfaces driven at relativistic intensity *Phys. Plasmas* **3** 3425
[19] Gibbon P 1996 Harmonic generation by femtosecond laser–solid interaction: a coherent water-window light source? *Phys. Rev. Lett.* **76** 50–3
[20] Baeva T, Gordienko S and Pukhov A 2006 Scalable dynamics of high energy relativistic electrons: theory, numerical simulations and experimental results *Astrophys. Space Sci.* **307** 335–40
[21] Dromey B *et al* 2009 Tunable enhancement of high harmonic emission from laser–solid interactions *Phys. Rev. Lett.* **102** 1–4
[22] Dromey B *et al* 2009 Diffraction-limited performance and focusing of high harmonics from relativistic plasmas *Nat. Phys.* **5** 146–52
[23] Quéré F, Thaury C, Monot P, Dobosz S, Martin P, Geindre J-P and Audebert P 2006 *Phys. Rev. Lett.* **96** 125004
[24] Aylward G and Findlay T 2002 *SI Chemical Data* (New York: Wiley)
[25] Conde M R 2004 Properties of aqueous solutions of lithium and calcium chlorides: formulations for use in air conditioning equipment design *Int. J. Therm. Sci.* **43** 367–82
[26] Faubel M 2000 Photoelectron spectroscopy at liquid surfaces *Adv. Ser. Phys. Chem.* **10** 634–90
[27] Lide D R 1992 *Handbook of Chemistry and Physics* 73rd edn (Boca Raton, FL: CRC Press) pp 6–14
[28] Murphy D M and Koop T 2005 Review of the vapor pressures of ice and supercooled water for atmospheric applications *Q. J. R. Meteorol. Soc.* **131** 1539–65
[29] Zepf M *et al* 1998 *Phys. Rev.* E **58** 5253
[30] Kahaly S *et al* 2013 *Phys. Rev. Lett.* **110** 175001
[31] Hirschfelder J O 1954 *Molecular Theory of Gases and Liquids* (New York: Wiley)